REPORT SSD-TR-89-88

CW Stimulated Brillouin Scattering of Long-Pulse Chemical Laser Beams

S. T. AMIMOTO and R. HOFLAND, JR.
Aerophysics Laboratory
Laboratory Operations
The Aerospace Corporation
El Segundo, CA 90245

15 November 1989

Prepared for

SPACE SYSTEMS DIVISION
AIR FORCE SYSTEMS COMMAND
Los Angeles Air Force Base
P.O. Box 92960
Los Angeles, CA 90009-2960

This report was submitted by The Aerospace Corporation, El Segundo, CA 90245, under Contract No. F04701-85-C-0086 with the Space Systems Division, P.O. Box 92960, Los Angeles, CA 90009-2960. It was reviewed and approved for The Aerospace Corporation by W. P. Thompson, Director, Aerophysics Laboratory.

Capt Scott W. Levinson was the project officer for the Mission-Oriented Investigation and Experimentation (MOIE) Program.

This technical report has been reviewed and is approved for publication. Publication of this report does not constitute Air Force approval of the report's findings or conclusions. It is published only for the exchange and stimulation of ideas.

SCOTT W. LEVINSON, CAPT, USAF
MOIE Project Officer
SSD/CNID

RAYMOND M. LEONG, MAJ, USAF
MOIE Program Manager
AFSTC/WCO OL-AB

UNCLASSIFIED

SECURITY CLASSIFICATION OF THIS PAGE

REPORT DOCUMENTATION PAGE

1a. REPORT SECURITY CLASSIFICATION Unclassified	1b. RESTRICTIVE MARKINGS
2a. SECURITY CLASSIFICATION AUTHORITY	3. DISTRIBUTION/AVAILABILITY OF REPORT Approved for public release; distribution unlimited.
2b. DECLASSIFICATION/DOWNGRADING SCHEDULE	
4. PERFORMING ORGANIZATION REPORT NUMBER(S) TR-0086A(2930-06)-1	5. MONITORING ORGANIZATION REPORT NUMBER(S) SSD-TR-89-88
6a. NAME OF PERFORMING ORGANIZATION The Aerospace Corporation Laboratory Operations 6b. OFFICE SYMBOL (If applicable)	7a. NAME OF MONITORING ORGANIZATION Space Systems Division
6c. ADDRESS (City, State, and ZIP Code) El Segundo, CA 90245	7b. ADDRESS (City, State, and ZIP Code) Los Angeles Air Force Base Los Angeles, CA 90009-2960
8a. NAME OF FUNDING/SPONSORING ORGANIZATION 8b. OFFICE SYMBOL (If applicable)	9. PROCUREMENT INSTRUMENT IDENTIFICATION NUMBER F04701-85-C-0086
8c. ADDRESS (City, State, and ZIP Code)	10. SOURCE OF FUNDING NUMBERS PROGRAM ELEMENT NO. / PROJECT NO. / TASK NO. / WORK UNIT ACCESSION NO.

11. TITLE (Include Security Classification)
CW Stimulated Brillouin Scattering of Long-Pulse Chemical Laser Beams

12. PERSONAL AUTHOR(S)
Amimoto, S. T., and Hofland, R. Jr.

13a. TYPE OF REPORT	13b. TIME COVERED	14. DATE OF REPORT (Year, Month, Day)	15. PAGE COUNT
	FROM _____ TO _____	1989 November 15	18

16. SUPPLEMENTARY NOTATION

17. COSATI CODES			18. SUBJECT TERMS (Continue on reverse if necessary and identify by block number)
FIELD	GROUP	SUB-GROUP	Photolysis laser HF chemical laser

19. ABSTRACT (Continue on reverse if necessary and identify by block number)

Backward Stimulated Brillouin Scattering (SBS) is currently under consideration as a nonlinear optical process for passive phase conjugation (beam clean up) phase matching (beam combination), and pointing and tracking of continuous-wave (CW) HF chemical lasers for high power applications. Theoretical considerations indicate, however, that forward SBS processes dominate over backward SBS phenomena in the steady-state limit, so that SBS exhibits the desired properties (phase conjugation) only for short time periods. Since backward SBS thresholds for CW HF lasers are about 0.20 MW per spectral line, long-pulse laboratory chemical laser sources (PCLs) are needed to investigate small-angle forward scattering phenomena and the development of techniques for their suppression. The laser data presented herein suggest that a moderate-volume, photolysis-pumped PCL is a suitable source for the study of steady-state forward SBS processes and their suppression. In particular, low pressure PCLs can simulate CW HF-laser SBS behavior under conditions of the proper pump bandwidth, laser spectrum, SBS media effects, longitudinal mode structure, and other high-power HF laser characteristics.

20. DISTRIBUTION/AVAILABILITY OF ABSTRACT	21. ABSTRACT SECURITY CLASSIFICATION
☒ UNCLASSIFIED/UNLIMITED ☐ SAME AS RPT ☐ DTIC USERS	Unclassified
22a. NAME OF RESPONSIBLE INDIVIDUAL	22b. TELEPHONE (Include Area Code) / 22c. OFFICE SYMBOL

DD FORM 1473, 84 MAR

83 APR edition may be used until exhausted.
All other editions are obsolete

SECURITY CLASSIFICATION OF THIS PAGE
UNCLASSIFIED

CONTENTS

FIGURES

I. INTRODUCTION

Experimental data are presented herein that show the dependence of DF chemical-laser pulse energy and pulse duration on cavity pressure for mixtures containing 20% F_2 and 8% D_2 by molar volume. The data indicate that DF-laser pulse energy E and pulse duration τ obey the approximate scaling relations $E \sim p^{+1/2}$, $\tau \sim p^{-3/4}$, and $E\tau \sim p^{-1/4}$, where p is the laser cavity pressure. The results are in sharp disagreement with the predictions of theoretical and analytical models of pulsed chemical lasers (PCLs) for which the product $E\tau$ is found to be invariant. Possible explanations for the observed anomalous behavior are noted at the conclusion of this report. The low pressure performance of a photolytically-pumped HF PCL is inferred from the present DF data and compared with the requirements for steady-state SBS. We conclude that a moderate energy PCL system of the type employed in the present investigation is a suitable device for the investigation of SBS processes appropriate to CW HF laser systems.

II. EXPERIMENTAL TECHNIQUE

The important features of the Aerospace photolysis laser system and associated diagnostics are described in Reference 1. Briefly, the laser reactor vessel is a quartz tube with walls 6 mm thick, an inside diameter of 9.15 cm, and a length of 100 cm. Positioned at equal intervals around the outer perimeter of the reactor vessel are four 1-m-long flashlamps that provide ultraviolet (UV) radiation to initiate the chain reaction between F_2 and $D_2(H_2)$. Cusp-shaped reflectors behind each flashlamp direct a portion of the light emitted from the lamp discharges into the quartz laser vessel. The laser windows are uncoated CaF_2 crystals, 12.5 cm in diameter and 1.9 cm thick, that are tilted with respect to the optical axis. Laser energy is extracted from the gain medium by means of a confocal, edge-coupled unstable resonator having an outcoupling fraction of 66%. Burn patterns on calibrated witness film reveal a reasonably uniform intensity profile in the near-field output beam. Far field beam quality is 1.1 times the diffraction limit as determined by power in the bucket measurements. The optical extraction volume of the photolysis laser is 5.78 ℓ.

A nonstandard electrical circuit is used to drive the four parallel flashlamps that initiate the photolysis laser. A 2.8 μF capacitor (Maxwell Laboratory type C) rated at 60 kV is used to energize the flashlamps. A spark gap (Physics International 675) is triggered to initiate the discharge. The lamps are connected to the output end of the switch by means of twelve RG-213 cables (three per lamp) that are 1.5 m long; a parallel arrangement is used to minimize the cable contribution to the total circuit inductance. The circuit inductance is dominated by that of the individual flashlamps and their close-coupled current returns. A coil (Pearson) placed on one of the ground returns from each lamp permits the current flow through all lamps to be monitored simultaneously. During circuit operation, resonance charging of the cables facilitates prompt breakdown of the flashlamps. A cable length of 3 m between lamps is found to be adequate to ensure synchronous firing of the four parallel lamps. Measured jitter between flashlamps is well within 100 ns. An RCA 1P28 photomultiplier with Corning 7-54 UV filter is used to monitor the UV output from all flashlamps.

A low-speed flow system is employed to meter and mix gases for use in the laser studies reported herein. Commercial-purity F_2 and O_2 are premixed at 5-10 atm pressure in a 76-ℓ passivated stainless-steel reservoir that has perforated stings to ensure good mixing. This mixture flows through a regulator and then to a mixer where it is injected through a calibrated sonic orifice. Metered flows of the remaining commercial-purity gases (D_2 or H_2 and SF_6, or He) are injected into the mixer through additional sonic orifices. An oxygen-rich mixture is used to fill the laser cavity to a pressure slightly above the first explosion limit. At this pressure, the laser chamber is purged with an oxygen-lean mixture that is subsequently used to complete the cavity fill to the desired final pressure. Gases from the laser device are exhausted by an 8500-ℓ/min mechanical vacuum pump to a two-stage KOH-water scrubber and an 84-m^3/min blower system. To prevent gross prereaction with nondilute mixtures during laser operation, the entire laser and plumbing interior must be carefully cleaned and passivated between laser shots.

Laser quantities that have been monitored in the present study are pulse energy, irradiance time history, near-field fluence distribution, and spectral output. The bulk of the laser pulse is transmitted through a CaF_2 wedge to a calibrated witness film upon which the near-field fluence distribution is impressed. The first wedge surface diverts about 3% of the total pulse energy to a ballistic thermopile having either a 9-cm or a 20-cm entrance aperture. The emission time history of the laser is monitored by means of a fast gold-doped-germanium (Au:Ge) detector that reads the reflection from the second wedge surface. Spectral measurements are also made on selected laser shots. The spectrometer consists of a 50 × 50 mm, 150 line/mm grating blazed at 4.0 μm, and a focusing mirror. The optical path leading to the grating is maintained free of all focusing elements; thus, a well-collimated input beam is delivered to the focusing mirror. A calibrated witness film, placed at the focus of the spectrometer exit mirror, provides the desired laser spectral information.

III. RESULTS AND DISCUSSION

The major experimental results of the present study are summarized in Figs. 1-3. In these figures, DF laser pulse energy E, FWHM pulse duration τ, and their product $E\tau$ are plotted as a function of laser cavity pressure p.

The data of Fig. 1, corresponding to 2.2% O_2, show DF laser pulse energy increasing from about 40-54 J at low pressures (100 Torr) to about 120-130 J at high pressures (700 Torr). The significant scatter in the low-pressure pulse energy data are caused by large fluctuations in the oxygen content during successive runs. (Refer to Fig. 4 where the strong sensitivity of laser output to O_2 concentration is illustrated.) No attempt was made to carry out lengthy purges that produce extremely low O_2 concentrations during the course of the present study. Had this been done, the absolute DF pulse energies would have been about 50% higher than the results presented in Fig. 1. (Compare, for example, the 200 J photolysis data at 1.3% O_2 and the 130 J photolysis data at 2.2% O_2 that are shown in Fig. 4.)

The data of Fig. 1 were obtained using a single unstable resonator of high magnification and high outcoupling (δ = 67%). The use of a high Q resonator of low outcoupling ($\delta \sim$ 10-20%) would have significantly enhanced laser performance at low cavity pressures. We estimate the performance increase using a high Q resonator to be about 20-30% in output laser energy and 20-30% in laser pulse duration.

The theory of Ref. 2 predicts that $E \sim (F/F_2)^{1/2}F_2$ in the present parameter regime. The 9 cm-bore photolysis laser is optically thin over the pressure range under consideration, so $(F/F_2)^{1/2} = C$. Since mixtures containing only 20% F_2 by molar volume are under consideration, $E \sim X_P p \sim p$ according to Ref. 2. The data of Fig. 1 indicate, however, that $E \sim p^{1/2}$, in sharp disagreement with the scaling law prediction of Ref. 2. (Note that limited comparisons with comprehensive numerical models have supported the scaling predictions of Ref. 2.) One possible source for the observed disagreement could be a fast prereaction at high pressures that depletes the reagent concentration and available output energy prior to initiation. A second cause

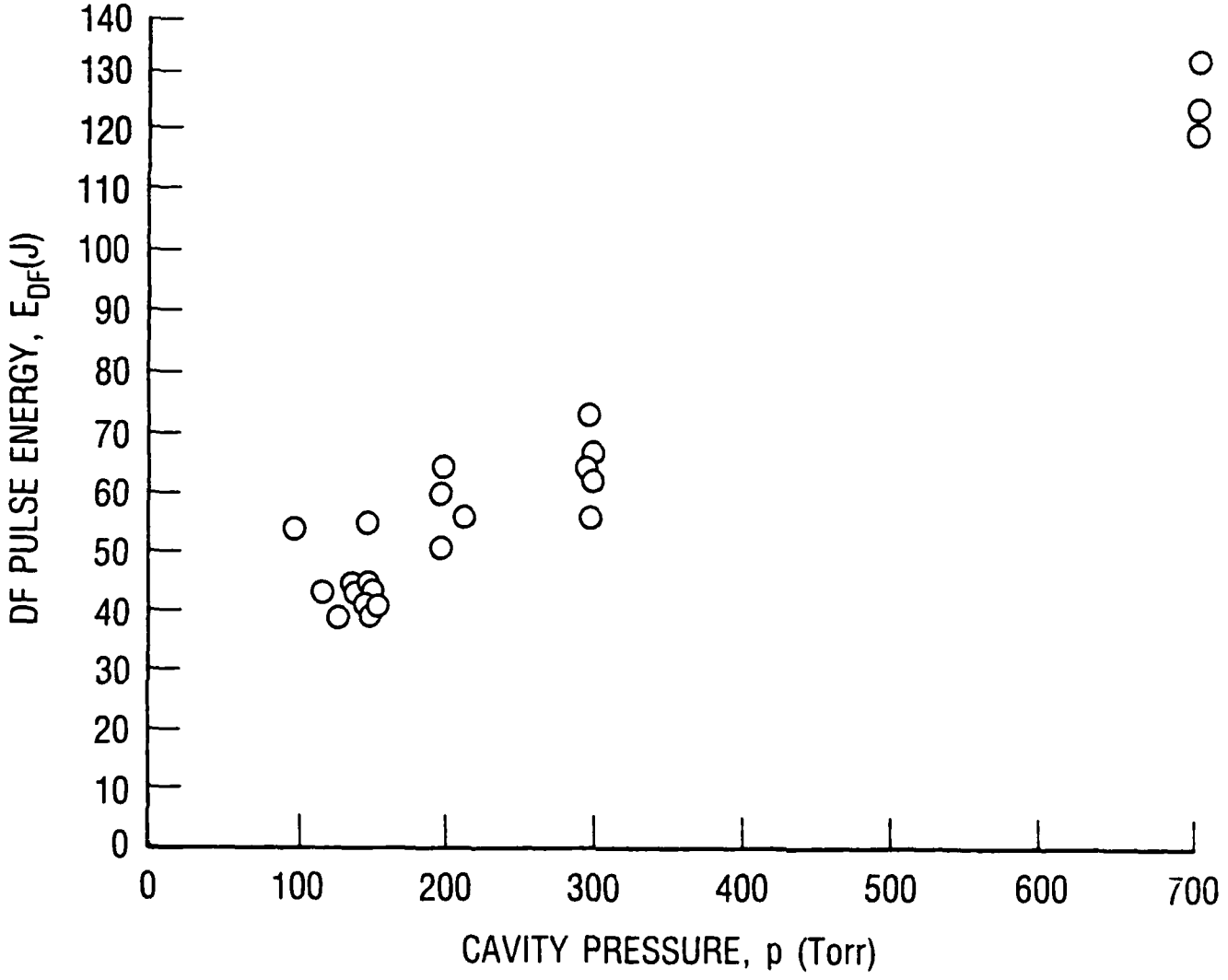

Fig. 1. DF-Laser Pulse Energy vs Cavity Pressure
($20\%F_2:8\%D_2:2.2\%O_2$, δ_{oc} = 67%)

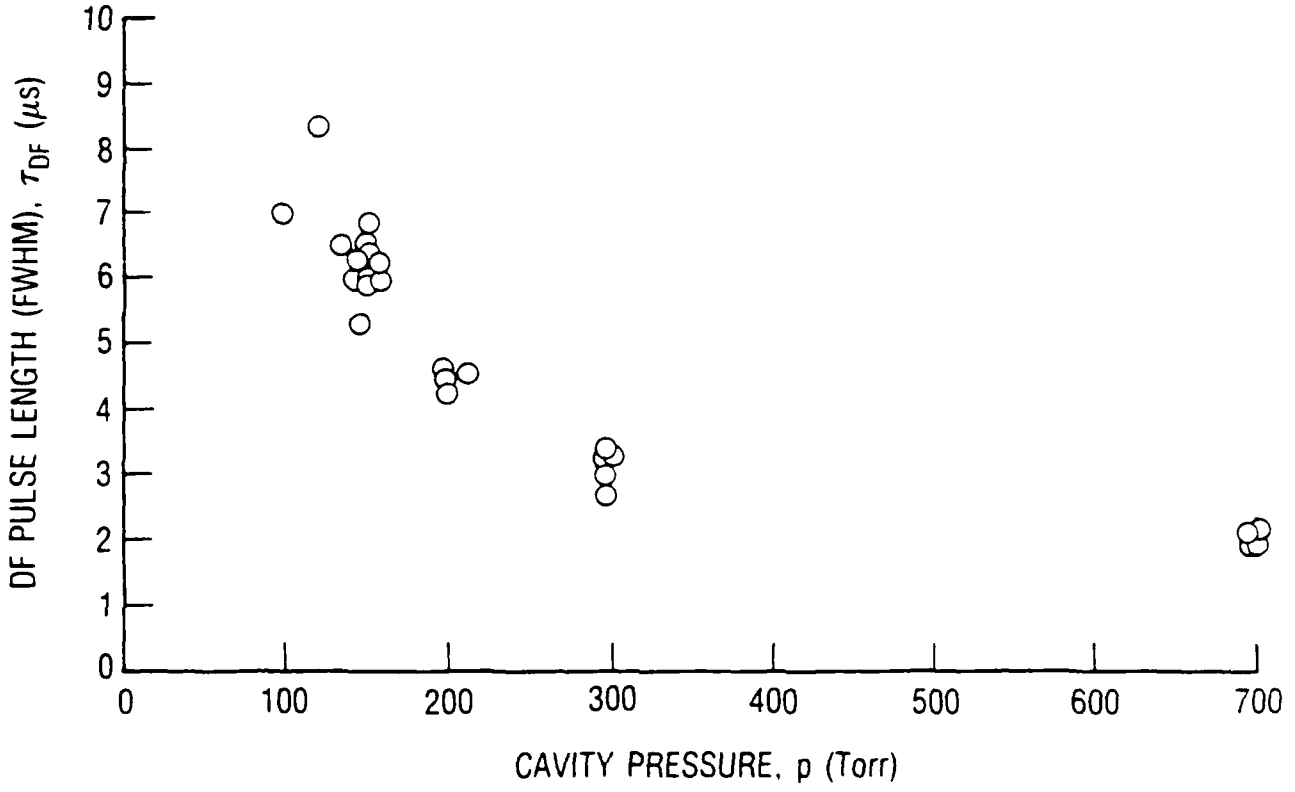

Fig. 2. DF-Laser Pulse Length vs Cavity Pressure ($20\%F_2:8\%D_2:2.2\%O_2$, δ_{oc} = 67%)

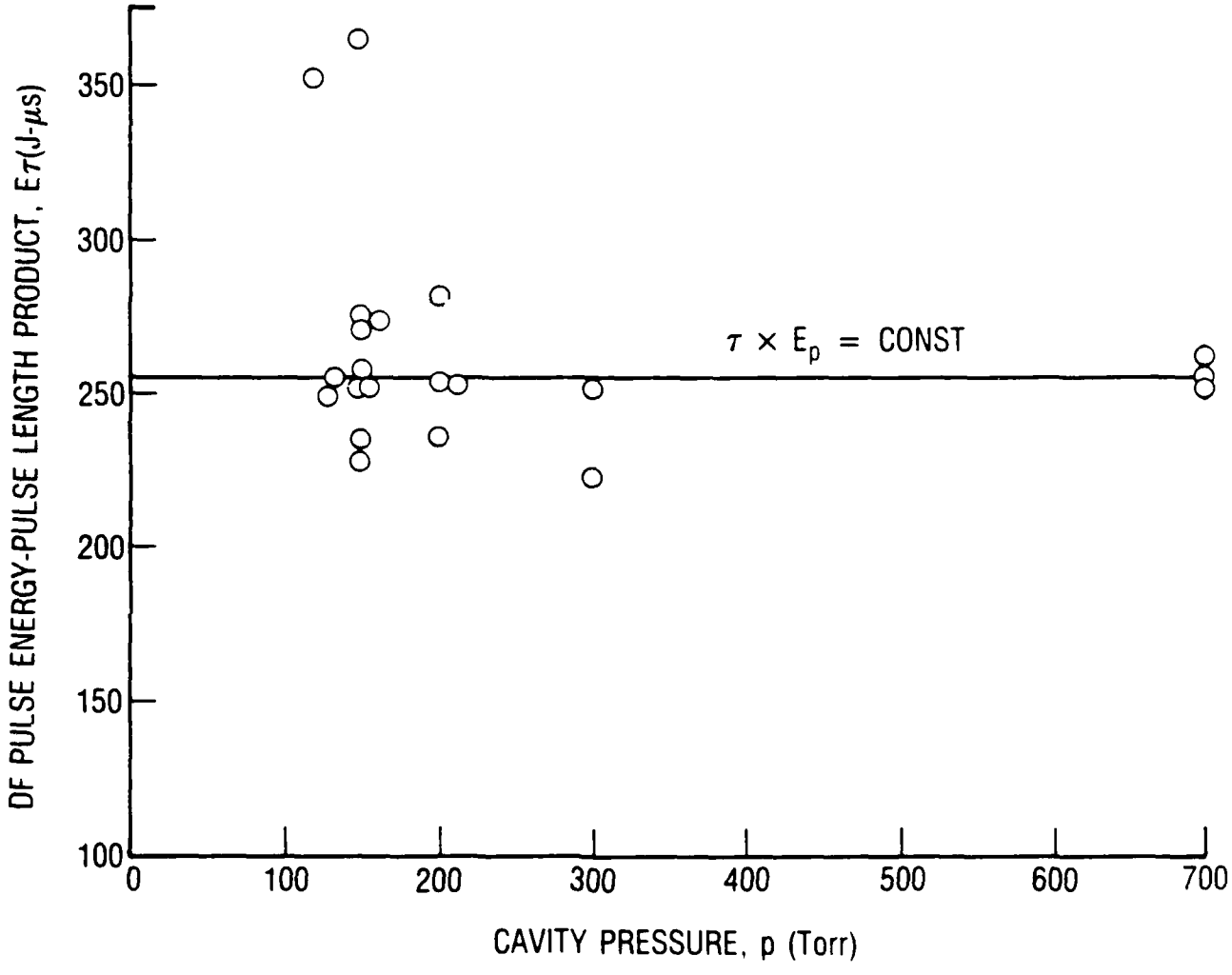

Fig. 3. DF-Laser Pulse Energy-Pulse Length Product vs Cavity Pressure ($20\%F_2:8\%D_2:2.2\%O_2$, δ = 67%)

for the discrepancy could be a fast three-body reaction that significantly degrades high pressure laser performance, but has negligible effect at low cavity pressures. Further theoretical and experimental studies are needed to resolve this scaling issue.

The effect of O_2 on laser performance for e-beam and flashlamp-initiated lasers is shown in Fig. 4. From these data, photolysis-initiated laser performance data at 800-Torr cavity pressure have been extracted and replotted in Fig. 5 for the case $(F/F_2)^{1/2}\ F_2 = 8$ Torr (equivalent to $F/F_2 = 0.25\%$). The effect of lowering O_2 from 2.2% to 1.3% is seen to be a 50% increase in laser output energy.

The photolysis laser output on the $P_2(8)$ line of HF is of initial interest in steady-state SBS investigations. The PCL output, when operated as an HF laser, can be obtained by multiplying the DF laser output energy by the factor 1.67 (Ref. 1). Experiments in our laboratory using an HF PCL have demonstrated that 20% of the total laser output can be extracted on the $P_2(8)$ line. Thus, DF pulse energy data of Fig. 1 can be scaled to the single line SBS case of interest using the relation

$$E_{HF}^{P_2(8)} = \frac{E_{P_2(8)}}{E_{HF}} \times \frac{E_{HF}}{E_{DF}} \times \frac{E_{1.30_2}}{E_{2.20_2}} \times \frac{E_{hiO}}{E_{lowO}} \times E_{DF}\ (\text{Fig. 1}) \qquad (1)$$

$$= 0.2 \times 1.67 \times 1.5 \times 1.2 \times D_{DF}^{\text{Fig. 1}} = 0.6\ E_{DF}^{\text{Fig. 1}}$$

The threshold laser energies necessary to achieve passive phase conjugation and laser beam combining by SBS have been derived for a pulsed HF laser and a xenon SBS medium as (Ref. 3)

$$E_{th}(J) = 8.7 \times 10^9\ \lambda^3(cm)\ \tau(\mu sec)\beta \qquad (2)$$

where $\lambda = 2.8$ μm is the laser wavelength, τ is the FWHM laser pulse width, and $\beta = 1.1$ is the laser beam quality. By Eq. (2), for a 10 μs HF laser pulse, the SBS threshold energy is calculated to be 2.1 J. With the Aerospace photolysis laser device operating on the H_2-F_2 chain reaction, a 10 μs dura-

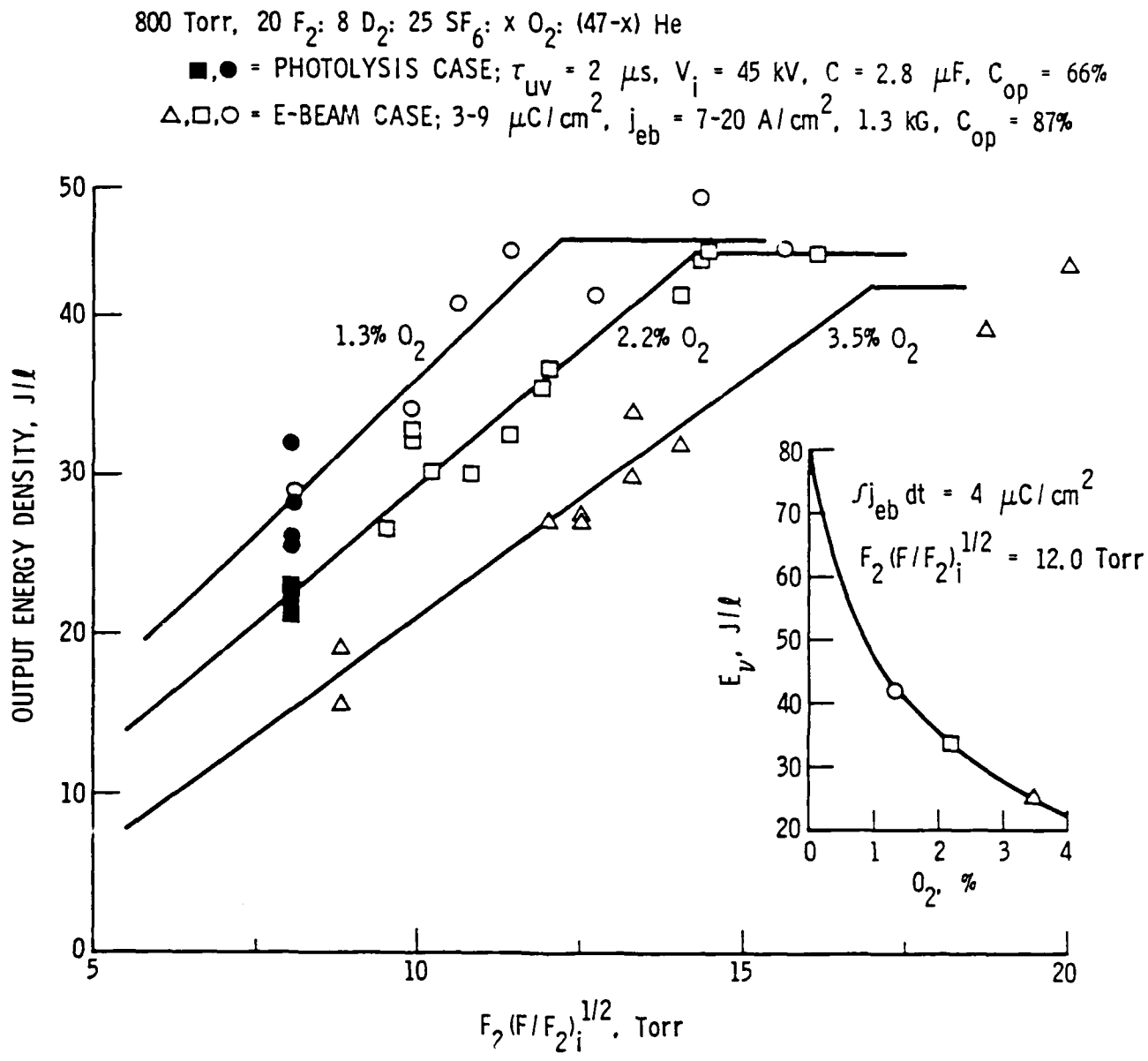

Fig. 4. DF Laser Specific Energy vs Scaling Parameter [Mixture = 20 F_2: 8 D_2: 25 SF_6: × O_2: (47-x) He, at 800 Torr.]

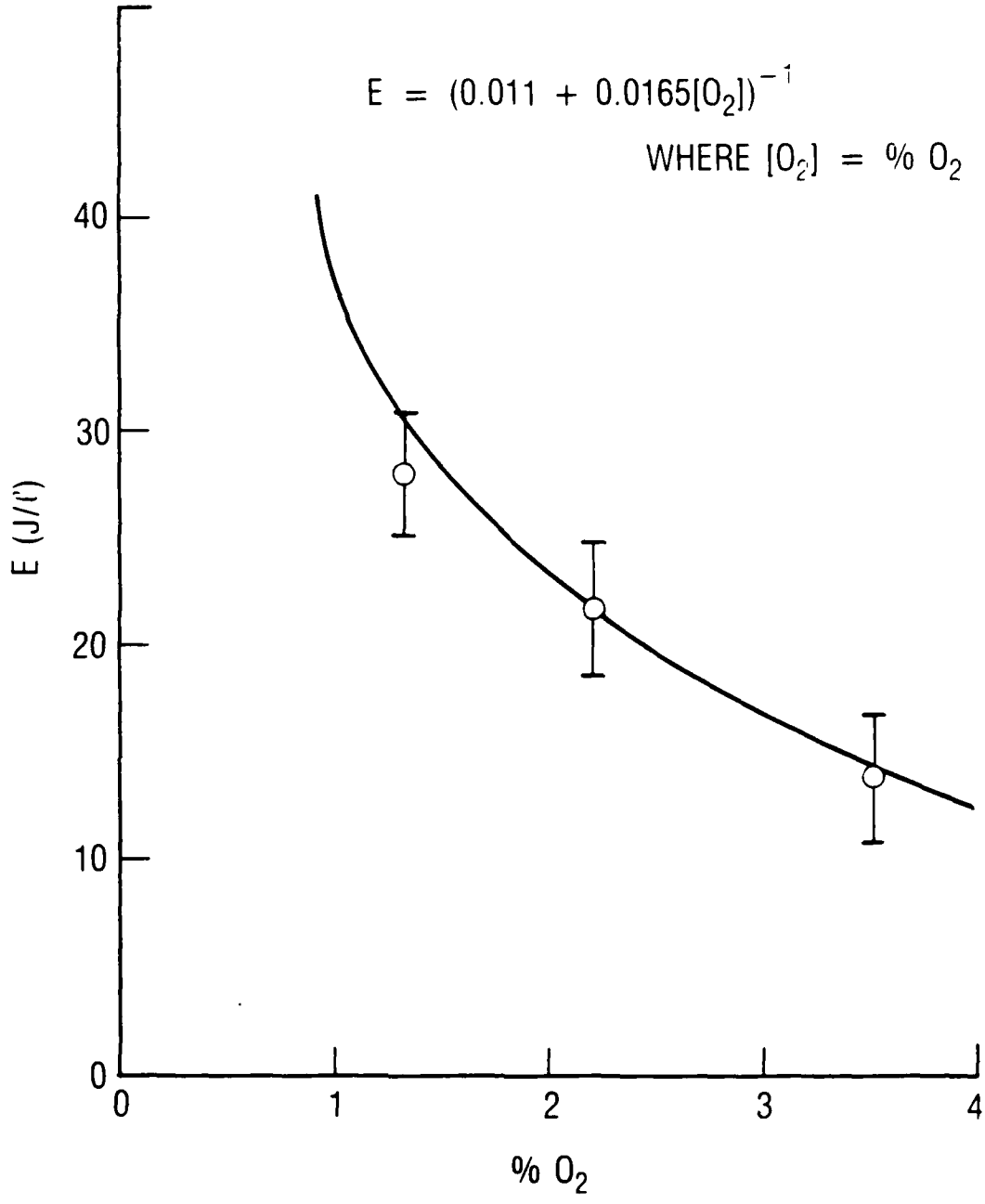

Fig. 5. Effect of O_2 on DF Laser Performance (800 Torr mix: 20% F_2; 8% D_2; 25% SF_6; 1.3 to 3.50% O_2; bal. He Initiation Level: F/F_2 = 0.25%)

tion laser pulse is sufficiently long to place one in a steady-state or CW SBS regime (Refs. 4, 5).

Reference to the DF-laser pulse length data of Fig. 2 indicates that 10 μs or longer pulses may be obtained at 100 Torr cavity pressures. (Here, the assumption is made that a high Q cavity is employed and that mixtures containing low O_2 concentrations are utilized.) To first order, the pulse lengths of HF and DF PCLs are found to be comparable for a given mixture composition, initiation level, cavity pressure, and resonator magnification, i.e.,

$$\tau_{HF}(X_i, \frac{F}{F_2}, p, M, \ldots) \simeq \tau_{DF}(X_i, \frac{F}{F_2}, p, m, \ldots) \qquad (3)$$

Reference to the DF pulse-energy data of Fig. 1 and to Eq. (1) indicates that at cavity pressures of 100 Torr, pulse energy densities of 4 J/liter or greater may be extracted on the $P_2(8)$ transition of an HF chemical laser.

IV. CONCLUSIONS

The major conclusions of this study are the following:

1. HF laser pulses of 10 μs or more can be extracted from photolysis-initiated chemical lasers operating in the neighborhood of 100 Torr cavity pressure; such HF pulses are long enough to investigate steady-state SBS phenomena in several important SBS media.

2. For the long pulse regime described in conclusion (1) above, moderate-volume (5 liter) photolysis lasers can produce single-line HF pulse energies that are an order of magnitude in excess of the SBS threshold for phase conjugation and beam combining.

3. The deviation of theoretical predictions from experimentally observed pressure scaling of PCLs is not understood at present; further studies are needed to resolve deficiencies in pulsed chemical laser theory.

4. A low pressure PCL can simulate CW HF-laser SBS behavior under conditions of the proper pump bandwidth, laser spectrum, SBS media effects, longitudinal mode structure, and other high-power HF laser characteristics.

REFERENCES

1. S. T. Amimoto, R. W. F. Gross, D. A. Durran, and R. Hofland, Aerospace Report SD-TR-83-102, 31 Jan. 1984 (to appear J. Appl. Phys.).

2. H. Mirels, R. Hofland, and J. S. Whittier, J. Appl. Phys. 50, 6660 (1979).

3. R. Hofland, "SBS Phase Conjugation Experiment," Aerospace ATM 86(6930-01)-01 (17 June 1986).

4. B. Ya. Zel dovich, et al., Principles of Phase Conjugation, Springer-Verlag, Berlin (1985).

5. T. Corvo, J. Glessner, and A. Gavrielides, "Forward Stimulated Brillouin Scattering," presented at SDIO Nonlinear Optics Workshop, Kirtland Air Force Base (28-31 Nov. 1986).

LABORATORY OPERATIONS

The Aerospace Corporation functions as an "architect-engineer" for national security projects, specializing in advanced military space systems. Providing research support, the corporation's Laboratory Operations conducts experimental and theoretical investigations that focus on the application of scientific and technical advances to such systems. Vital to the success of these investigations is the technical staff's wide-ranging expertise and its ability to stay current with new developments. This expertise is enhanced by a research program aimed at dealing with the many problems associated with rapidly evolving space systems. Contributing their capabilities to the research effort are these individual laboratories:

Aerophysics Laboratory: Launch vehicle and reentry fluid mechanics, heat transfer and flight dynamics; chemical and electric propulsion, propellant chemistry, chemical dynamics, environmental chemistry, trace detection; spacecraft structural mechanics, contamination, thermal and structural control; high temperature thermomechanics, gas kinetics and radiation; cw and pulsed chemical and excimer laser development including chemical kinetics, spectroscopy, optical resonators, beam control, atmospheric propagation, laser effects and countermeasures.

Chemistry and Physics Laboratory: Atmospheric chemical reactions, atmospheric optics, light scattering, state-specific chemical reactions and radiative signatures of missile plumes, sensor out-of-field-of-view rejection, applied laser spectroscopy, laser chemistry, laser optoelectronics, solar cell physics, battery electrochemistry, space vacuum and radiation effects on materials, lubrication and surface phenomena, thermionic emission, photosensitive materials and detectors, atomic frequency standards, and environmental chemistry.

Computer Science Laboratory: Program verification, program translation, performance-sensitive system design, distributed architectures for spaceborne computers, fault-tolerant computer systems, artificial intelligence, microelectronics applications, communication protocols, and computer security.

Electronics Research Laboratory: Microelectronics, solid-state device physics, compound semiconductors, radiation hardening; electro-optics, quantum electronics, solid-state lasers, optical propagation and communications; microwave semiconductor devices, microwave/millimeter wave measurements, diagnostics and radiometry, microwave/millimeter wave thermionic devices; atomic time and frequency standards; antennas, rf systems, electromagnetic propagation phenomena, space communication systems.

Materials Sciences Laboratory: Development of new materials: metals, alloys, ceramics, polymers and their composites, and new forms of carbon; nondestructive evaluation, component failure analysis and reliability; fracture mechanics and stress corrosion; analysis and evaluation of materials at cryogenic and elevated temperatures as well as in space and enemy-induced environments.

Space Sciences Laboratory: Magnetospheric, auroral and cosmic ray physics, wave-particle interactions, magnetospheric plasma waves; atmospheric and ionospheric physics, density and composition of the upper atmosphere, remote sensing using atmospheric radiation; solar physics, infrared astronomy, infrared signature analysis; effects of solar activity, magnetic storms and nuclear explosions on the earth's atmosphere, ionosphere and magnetosphere; effects of electromagnetic and particulate radiations on space systems; space instrumentation.